

Stochastic bimodalities in deterministically monostable reversible chemical networks due to network topology reduction

Maxim N. Artyomov,¹ Manikandan Mathur,² Michael S. Samoilov,³ and Arup K. Chakraborty^{1,4,5,a)}

¹*Department of Chemistry, Massachusetts Institute of Technology, Cambridge, Massachusetts 02139, USA*

²*Department of Mechanical Engineering, Massachusetts Institute of Technology, Cambridge, Massachusetts 02139, USA*

³*QB3: California Institute for Quantitative Biosciences, University of California, Berkeley, California 94720, USA and Physical Biosciences Division, Lawrence Berkeley National Laboratory, Berkeley, California 94720, USA*

⁴*Department of Chemical Engineering, Massachusetts Institute of Technology, Cambridge, Massachusetts 02139, USA*

⁵*Department of Biological Engineering, Massachusetts Institute of Technology, Cambridge, Massachusetts 02139, USA*

(Received 5 August 2009; accepted 22 October 2009; published online 19 November 2009)

Recently, stochastic simulations of networks of chemical reactions have shown distributions of steady states that are inconsistent with the steady state solutions of the corresponding deterministic ordinary differential equations. One such class of systems is comprised of networks that have irreversible reactions, and the origin of the anomalous behavior in these cases is understood to be due to the existence of absorbing states. More puzzling is the report of such anomalies in reaction networks without irreversible reactions. One such biologically important example is the futile cycle. Here we show that, in these systems, nonclassical behavior can originate from a stochastic elimination of all the molecules of a key species. This leads to a reduction in the topology of the network and the sampling of steady states corresponding to a truncated network. Surprisingly, we find that, in spite of the purely discrete character of the topology reduction mechanism revealed by “exact” numerical solutions of the master equations, this phenomenon is reproduced by the corresponding Fokker–Planck equations. © 2009 American Institute of Physics.

[doi:10.1063/1.3264948]

Diverse cellular functions are mediated by signal transduction and subsequent gene transcription events. The dynamical behavior of chemical reaction networks control and regulate these processes. The dynamics of spatially homogeneous chemical reactions are often described by deterministic ordinary differential equations in terms of classical chemical kinetics (CCK).^{1,2} The mean-field character of such a treatment is exemplified by considering the following deterministic ordinary differential equation describing the dynamics of second order reactions such as $A + B \xrightarrow{k} AB$:

$$-d\langle A \rangle / dt = k\langle A \cdot B \rangle \approx k\langle A \rangle \langle B \rangle, \quad (1)$$

where k is the rate coefficient. In writing Eq. (1), the number of molecules of each species is described by an average concentration ($\langle A \rangle$ or $\langle B \rangle$) and the average of the product of the number of A and B molecules is replaced by the product of the average concentrations. In other words, stochastic and discrete features of the underlying molecular number levels, including fluctuations and associated correlations are ignored.

Cell signaling and gene transcription often involve small copy numbers of the pertinent molecules. Therefore, many important examples of stochastic fluctuations in determining

cellular response have been reported.^{3–5} Accurate analysis of these and other chemical processes—for which the underlying discrete molecular states or random nature of individual interactions become important—requires methods able to capture such features. This is frequently done via the chemical master equation (CME).⁶

For example, when a continuous-deterministic CCK description of the dynamics of chemical reactions yields multiple steady states in some parameter range, the corresponding discrete-stochastic CME descriptions will generally produce a multimodal distribution of responses. This is because CCK closely follows modes of the underlying CME distribution, so presence of multiple steady states under the same set of parameters broadly indicates existence of multiple distribution modes.⁷ Notably, CME distributions with this type of multimodality, e.g., bimodality with cells being either “on” or “off,” can be realized for parameter ranges where a deterministic multi/bistability is predicted as well as outside of these regimes. The latter phenomenon results from stochastic sampling of parameters or dynamic states in the deterministically bistable regime, which is enabled by the fluctuations inherent in CME system trajectories that are not available under CCK.

A more intriguing class of phenomena is comprised of studies showing the existence of bimodal stochastic responses for systems whose deterministic description yields

^{a)}Electronic mail: arupc@mit.edu.

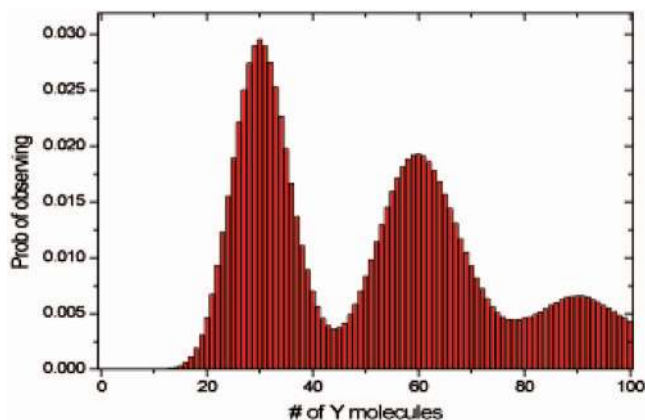


FIG. 1. Stochastic simulations for networks (1) and (2) with parameters $k_X=0.01$, $k_{-X}=0.01$, $k_Y=300$, and $k_{-Y}=10$. Steady-state distribution of molecules Y is shown.

monostable solutions for all parameter ranges. Two types of reaction networks in this class have been reported. One is comprised of systems with absorbing states (i.e., systems comprised of irreversible chemical reactions). It was recently demonstrated that the necessary and sufficient conditions for such a system to exhibit purely stochastic bimodal responses are the existence of more than one absorbing state and feedback loops characterized by distinct time scales.⁴ One interesting account attempting to unify considerations of chemical networks subject to fluctuations and time-scale separations has been published recently.⁸ The focus of this paper is on chemical reaction networks without absorbing states, e.g., networks comprised of reversible chemical reactions, which exhibit bimodal stochastic responses when a deterministic treatment is devoid of instabilities in any parameter range.

An example of such a system is obtained by considering the following simple birth-death process for a species X:^{9,10}



The rate constants in Eq. (2) can be chosen such that at steady state there are only few molecules of X present. This reaction can then be coupled to a fast “indicator” reaction as shown below:



Species X gives birth to species Y with rate k_Y , and Y can be degraded with the rate k_{-Y} . If the rate constants k_Y and k_{-Y} are chosen to be much larger than k_X and k_{-X} , an adiabatic concentration of Y is established corresponding to the particular value of X being sampled stochastically. When a small number of X molecules is present, on average, one can see the signature of the discreteness of X in multiple peaks appearing in the steady-state probability distribution of Y (see Fig. 1, simulations carried out with standard Gillespie algorithm¹¹), provided that the rates of the reactions (3) are fast enough that peaks in the steady-state distribution of Y are resolved. The “indicator reaction” effectively amplifies the discrete nature of the molecules of X which is why this scenario can be called the “discreteness amplification” sce-

nario for obtaining multip peaked distributions for deterministically monostable systems. A particular example of this scenario that was presented in Ref. 9 can be obtained from the reaction schemes (2) and (3) by restricting possible numbers of X molecules to zero or one. Referring to the state with $X=0$ as the inactive state of a gene and $X=1$ as the active state, a bimodal distribution of cellular response is obtained for conditions where the adiabatic limit is approached.

Our focus is on a different class of chemical reaction networks without absorbing states that can exhibit purely stochastic bimodalities. Kinetic schemes in this class have been described previously,¹² but the underlying reason for a bimodal stochastic response in the absence of any deterministic instabilities remained unclear. Here, we show that a previously unreported phenomenon, network topology reduction, is one of the mechanisms that could result in this unusual behavior.

We start by considering the following simple chemical reaction network:



The deterministic kinetic equations for this system are

$$\frac{dN}{dt} = -k_1 N^2 + k_2 NA - k_3 N + k_4 A,$$

$$\frac{dA}{dt} = k_1 N^2 - k_2 NA + k_3 N - k_4 A - k_5 A + k_6 B, \quad (6)$$

$$\frac{dB}{dt} = k_5 A - k_6 B.$$

Equation (6) makes clear that the quadratic equation obtained for steady-state concentrations of A (or B) can only result in a single stable fixed point for all possible values of the rate parameters. Stochastic simulation of this reaction network for some choices of parameter values, however, yields a bimodal response for the number of B molecules (Fig. 2). This phenomenon cannot be explained by the arguments described above in the “amplification of discreteness” scenario.

One of the peaks in the bimodal distribution in Fig. 2 corresponds to the monostable deterministic steady state solution of Eq. (6), but the other is different. The explanation for this unexpected stochastic bimodality can be found by considering the time courses of the concentrations of N and B simultaneously (Fig. 2, inset). One notices that values of B corresponding to the peak that is not centered around the deterministic solution (i.e., $B \sim 27$) are sampled when the number of molecules of N in the system accidentally, by way of stochastic fluctuations, becomes zero. In this situation, the

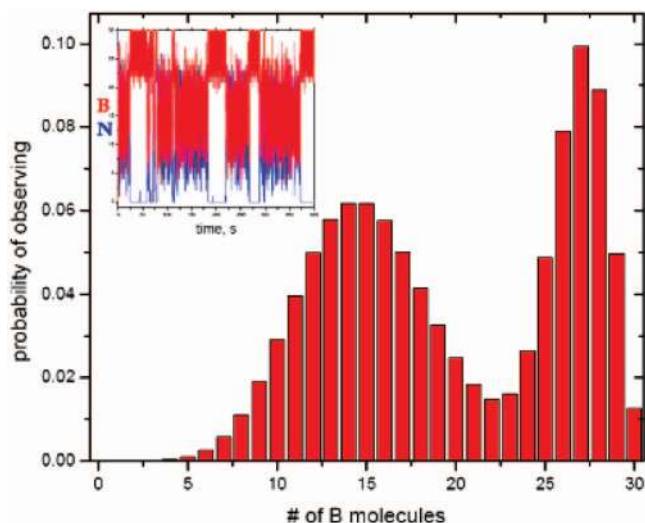


FIG. 2. Stochastic Simulations of the networks (3) and (4) with parameters $k_1=0.1$; $k_2=10$; $k_3=13$; $k_4=0.03$; $k_5=100$; $k_6=10$; and $N+A+B=30$. Steady-state distribution of molecules B is shown. Peak at $B\sim 27$ corresponds to steady-state of reduced network, while peak at $B\sim 15$ corresponds to steady state of the complete network. Inset: time course of simulations shown for N (red) and B (black) species.

reaction network effectively reduces in size because all reactions, where N is among the reactants cannot occur, which leads to certain kinetic degrees of freedom otherwise available to the system to be temporarily “frozen out,” subsequently constraining it onto a smaller dynamical manifold. The latter may potentially display different temporal or stationary features, thus contributing another behavioral mode to discrete-stochastic reaction network properties that may then be reflected in the overall species state distribution.

While a general analytical investigation of specific CME mechanisms underlying such phenomena is substantially outside the scope of this work and would need to be further addressed/discussed elsewhere, the described mechanism provides a compelling example of how this type of deviant chemical and biochemical dynamics can arise even in seemingly simple reaction mechanisms, making them relevant for *in vivo* and *in vitro* applications. For example, of the six reactions in the scheme described by Eqs. (4) and (5) only three are still possible if N is eliminated. If parameters are chosen appropriately, this reduced network may be realized for a sufficient amount of time to allow sampling of its steady state, with the second peak in the bimodal response shown in Fig. 2 corresponding to it. The only way for the system to escape from being “trapped” or “frozen” in the reduced network is through the occurrence of a reaction that produces N , i.e., the one that converts A to N here.

Another notable case of stochastic bimodality in a reversible chemical system has been considered by Samoilov *et al.*¹² and by Miller and Beard¹³ in the much-studied and biochemically ubiquitous futile cycle,^{1,3} which interconverts X and X^* with the help of enzymes E_+ and E_- according to the standard Michaelis–Menten mechanism, with E_+ subject to noise (9):

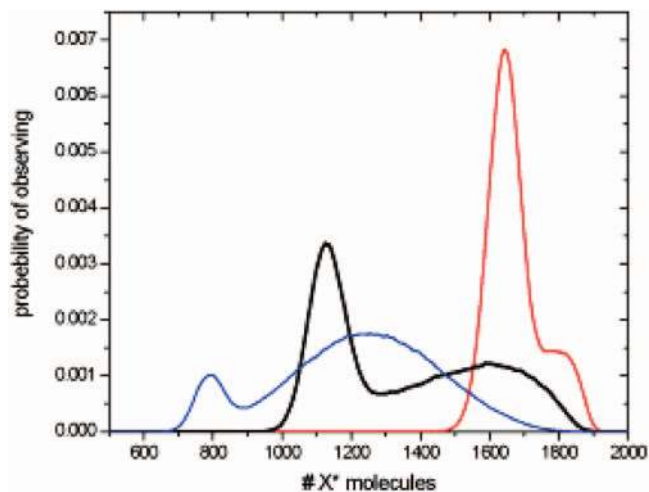
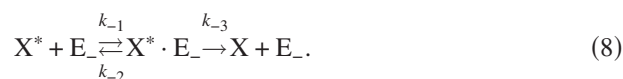
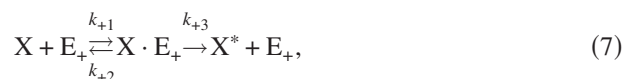
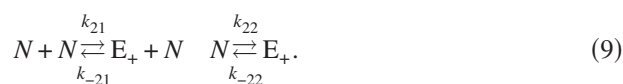


FIG. 3. Steady-state probability distribution, for the reaction networks (7)–(9) with parameters $k_1=40$; $k_2=10^4$; $k_3=10^4$; $k_{-1}=200$; $k_{-2}=100$; $k_{-3}=5000$; $k_{21}=10$; $k_{-21}=5$; $k_{22}=10$; $k_{-22}=0.2$; $X+X^*=2000$; and $E_-=50$ (same as Ref. 12) and $E_++N=30$ (red), $E_++N=35$ (black), and $E_++N=40$ (blue).



In Ref. 12, it has been shown that inducing a particular class of monomodal stationary distributions on the forward enzyme E_+ in the Michaelis–Menten regime may cause this deterministically monostable (for all parameter ranges¹⁴) process to undergo a noise-induced bifurcation, with the ensuing system response resulting in a bimodal distribution on X and X^* . While such deviant behavior could potentially be brought about by a range of external processes imparting the prescribed distribution on E_+ , the specific example considered in (12) achieved the required nonlinearity of noise appearing in the system of reactions (7) and (8) by having it coupled to a “noise generator” reaction mechanism of type (4) (or reaction (9) below)



The deterministic steady-state equations for the reaction system (7)–(9) are polynomials of up to sixth order and it is not straightforward to show that there is no bistability for *all* possible sets of rate constants. This can be circumvented by using the topological rules described by Feinberg and co-workers,¹⁵ which allow us to conclude that the system cannot admit more than one positive steady-state, regardless of parameter values. However, a bimodal steady-state distribution of X (and X^*) was found in Ref. 12 for a fully discrete-stochastic description of this chemical network in a narrow range of parameters (Fig. 3). Just like in the simple example considered previously, the behavior of the generator

reaction (9) may be viewed as having two network topologies. For nonzero values of N , the complete network (7)–(9) is explored and a peak around its steady state solution emerges. However, when the number of molecules of N stochastically becomes zero—the effective topology is reduced similar to that of mechanism (4) and (5) (see Fig. 3).

The necessary conditions for observing bimodality due to network topology reduction is that the steady-states for complete and reduced topologies are sufficiently different so that two distinct peaks can be resolved. The other necessary condition is that the system stays “arrested” in the reduced topology for a time scale sufficient for sampling its steady state. Samoilov *et al.*¹² may have achieved this for the driver reaction (9) by “kinetically” arresting the system in the reduced topology by setting k_{-22} Eq. (9) to be smaller than reaction rates pertinent for the reduced network (7) and (8). Since reaction k_{-22} is the only possible way to return from the reduced topology to the complete network, this kinetic restriction fulfils the second necessary requirement.

The strong constraints on the possible range of system parameters able to support the bimodality observed by Samoilov *et al.*¹² could be related to the violation of the second necessary condition above, which requires that the system be able to spend sufficient time in the $N=0$ state and that is possible only for a relatively small number of N molecules in the steady-state. Therefore, the observed bimodality disappears in Samoilov *et al.*¹² when increasing the number of molecules of N participating in the reaction. For $N+E_+=40$, the peak around $X=790$ corresponding to reduced topology

becomes very small compared with the situation when $N+E_+=35$ (Fig. 3). In spite of the fact that the peaks are well separated, the reduced topology is rarely sampled because fluctuations leading to $N=0$ are rare and the time spent in this state is short when N_{tot} is large.

When decreasing the number of molecules of N in the system, steady-state concentrations for complete and reduced topologies are very close to each other, and cannot be resolved in the simulation. For $N+E_+=35$, one sees two distinct peaks corresponding to $X=1602$ (complete system) and $X=1120$ (reduced topology). However, for $N+E_+=30$, steady-states for the full and reduced topologies are $X=1766$ and $X=1639$, respectively. These peaks cannot be resolved completely due to intrinsic noise of the level ± 70 molecules at steady-state conditions (Fig. 3). With further decrease in concentration, the two peaks merge into one.

We next turn to the possibility of treating systems of this type with continuous approximation methods, particularly the Fokker–Planck equation. The interest is stimulated by the fact that bimodality in this class of systems occurs due to special behavior at the single point where $N=0$. Is $N=0$ still a special point when N can take on noninteger values in a continuous approximation?¹⁶ For arbitrary small N , as long as it is not exactly 0, the effective topology is still the complete topology of the network, and the effect of the second attractor is not obvious.

Consider again the simplest kinetic schemes (4) and (5) featuring the network-topology reduction induced bimodality. The corresponding master equation

$$\begin{aligned} \frac{dP_{n,a,b}(t)}{dt} = & -\{k_1n(n-1) + k_2na + k_3n + k_4a + k_5a + k_6b\}P_{n,a,b}(t) + k_1n(n+1)P_{n+1,a-1,b}(t) + k_2(a+1)(n-1)P_{n-1,a+1,b}(t) \\ & + k_3(n+1)P_{n+1,a-1,b}(t) + k_4(a+1)P_{n-1,a+1,b}(t) + k_5(a+1)P_{n,a+1,b-1}(t) + k_6(b+1)P_{n,a-1,b+1}(t), \end{aligned} \quad (10)$$

can be transformed into a Fokker–Planck equation according to standard rules,¹⁶ and after taking care of conservation of mass law $n+a+b=T$ becomes

$$\begin{aligned} \frac{\partial P(n,a,t)}{\partial t} = & \frac{\partial}{\partial n}[f_1(n,a)P(n,a,t)] + \frac{\partial}{\partial a}[f_2(n,a)P(n,a,t)] \\ & + \frac{1}{2} \frac{\partial^2}{\partial n^2}[f_3(n,a)P(n,a,t)] \\ & + \frac{\partial^2}{\partial a \partial n}[f_4(n,a)P(n,a,t)] \\ & + \frac{1}{2} \frac{\partial^2}{\partial a^2}[f_5(n,a)P(n,a,t)], \end{aligned} \quad (11)$$

with

$$\begin{aligned} f_1 &= k_1n^2 - k_2na + k_3n - k_4a, \\ f_2 &= -k_1n^2 + k_2na - k_3n + k_4a + k_5a - k_6(T-a-n), \\ f_3 &= k_1n^2 + k_2na + k_3n + k_4a, \\ f_4 &= -k_1n^2 - k_2na - k_3n - k_4a, \\ f_5 &= k_1n^2 + k_2na + k_3n + k_4a + k_5a + k_6(T-a-n). \end{aligned} \quad (12)$$

The time dependent partial differential Eq. (10) was solved numerically with reflecting boundary conditions and the steady state distribution was determined in the very long time limit. In Fig. 4 the numerical solution of the Fokker–Planck equation is shown along with the steady-state distribution obtained from the stochastic simulations. Two virtually coinciding curves represent smoothed probability histogram at steady state. The height of the surface at point with coordinates A and N (both integer) is the probability of

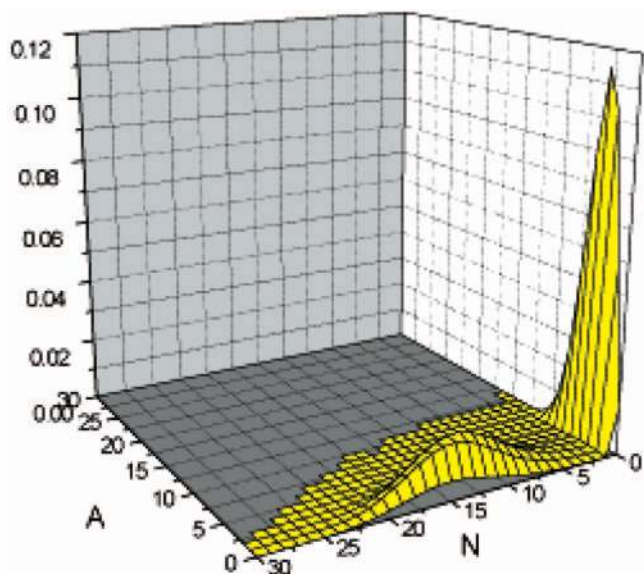
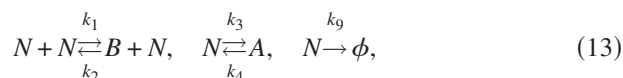


FIG. 4. Numerical solution of the Fokker–Planck Eq. (10) at infinite time, coinciding with results of stochastic simulations for networks (11) and (12) with the same parameters as Fig. 3 and $E_+ + N = 30$. Numerical solution was discretized as explained in the text in order to compare it with results of stochastic simulations.

having A and N molecules at steady state. In order to plot numerical solution of the Fokker–Planck equations in this manner, the continuous function $P(a, n)$ was binned into discrete probabilities [e.g., $P(A=2, N=5) = \int_{1.5}^{2.5} da \int_{4.5}^{5.5} dn P(a, n)$]. One can see immediately that continuous approximation correctly reproduces network topology reduction effects. An analogy can be drawn with diffusion on a surface where there is a pointlike sink to understand why the Fokker–Planck equation reproduces behavior that appears to arise from discreteness. Even if the surface is curved such that the mass is concentrated well away from the sink, in the very-long time limit the mass will escape through the sink due to negligible, but still nonzero, diffusive motion. The described Fokker–Planck equation has the character of diffusion in a potential well with an additional “finite” pointlike sink at the boundary.

Finally, it can be argued that the fact that both systems (4), (5), and (7)–(9) are “closed” and strictly obeying conservation of mass introduces additional nonlinearity at the boundary that is necessary to observe the mechanism of network topology reduction. In order to address this point we have constructed an “open” system that exhibits stochastically bimodal distribution due to topology reduction



As one can see from the Fig. 5, two peaks are observed in the steady-state histogram of B molecules. First peak at $B \sim 37$ molecule correspond to the complete network when both Eqs. (13) and (14) are dictating steady-state of the network. The second peak at $B \sim 91$ molecule correspond to the

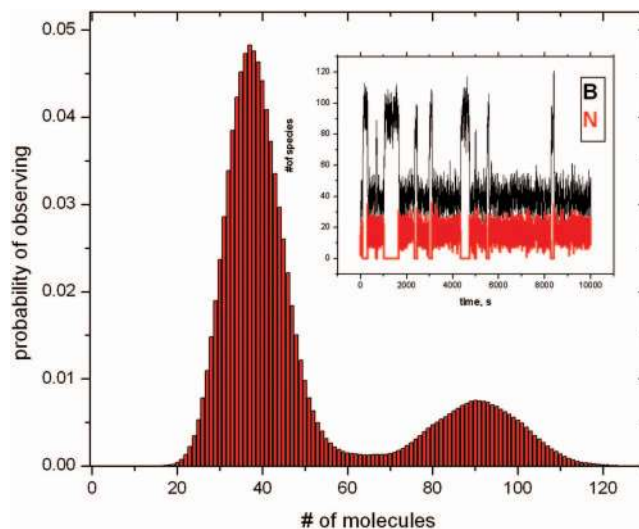


FIG. 5. Stochastic Simulations of the networks (13) and (14) with parameters $k_1=1$; $k_2=10$; $k_3=13$; $k_4=0.01$; $k_5=100$; $k_6=10$; $k_7=1$; $k_8=9$; and $k_9=0.4$. Steady-state distribution of molecules B is shown. Inset: time course of simulations shown for N (red) and B (black) species.

steady-state of the reduced network which consists only of Eq. (14). The second peak is observed when number of molecules of N stochastically goes to zero (see inset of Fig. 5).

In this work we have identified the mechanism that allows multi-peaked steady-state distributions for systems without absorbing states characterized by a single deterministic attractor (e.g., chemical networks consisting of purely reversible chemical reactions that have single stable solution for their ordinary differential equations chemical equations). This mechanism can be realized in both closed, mass-conserving system and in open, steady-state systems. The network topology reduction relies on the stochastic fluctuations in the particular network architectures that allow effective reduction in the number of possible reactions due to exhaust of one of the components. The validity of continuous (Fokker–Planck) description of this mechanism was also studied.

We would like to acknowledge helpful discussions with Jayajit Das, Jason Locasale, and Adam Arkin. Funding provided through NIH Director’s Pioneer Award to A.K.C. and Contract No. IPO1/AI071195/01 (A.K.C.).

¹ A. Goldbeter and D. E. Koshland, *Proc. Natl. Acad. Sci. U.S.A.* **78**, 6840 (1981); C. Gomez-Urbe, G. C. Verghese, and L. A. Mirny, *PLoS Comput. Biol.* **3**, e246 (2007).

² K. Lai, M. J. Robertson, and D. V. Schaffer, *Biophys. J.* **86**, 2748 (2004); N. I. Markevich, J. B. Hoek, and B. N. Kholodenko, *J. Cell Biol.* **164**, 353 (2004).

³ O. G. Berg, J. Paulsson, and M. Ehrenberg, *Biophys. J.* **79**, 1228 (2000); J. Levine, H. Y. Kueh, and L. Mirny, *ibid.* **92**, 4473 (2007).

⁴ M. N. Artyomov, J. Das, M. Kardar, and A. K. Chakraborty, *Proc. Natl. Acad. Sci. U.S.A.* **104**, 18958 (2007).

⁵ T. B. Kepler and T. C. Elston, *Biophys. J.* **81**, 3116 (2001).

⁶ D. A. McQuarrie, *J. Appl. Probab.* **4**, 413 (1967).

⁷ M. S. Samoilov and A. P. Arkin, *Nat. Biotechnol.* **24**, 1235 (2006).

⁸ H. Qian, P. Z. Shi, and J. H. Xing, *Phys. Chem. Chem. Phys.* **11**, 4861 (2009).

⁹ A. Lipshtat, A. Loinger, N. Q. Balaban, and O. Biham, *Phys. Rev. Lett.* **96**, (2006).

¹⁰ A. Loinger, A. Lipshtat, N. Q. Balaban, and O. Biham, *Phys. Rev. E* **75**,

(2007).

¹¹D. T. Gillespie, *J. Phys. Chem.* **81**, 2340 (1977).

¹²M. Samoilov, S. Plyasunov, and A. P. Arkin, *Proc. Natl. Acad. Sci. U.S.A.* **102**, 2310 (2005).

¹³C. A. Miller and D. A. Beard, *Biophys. J.* **95**, 2183 (2008).

¹⁴L. M. Wang and E. D. Sontag, *J. Math. Biol.* **57**, 29 (2008).

¹⁵G. Craciun, Y. Z. Tang, and M. Feinberg, *Proc. Natl. Acad. Sci. U.S.A.* **103**, 8697 (2006).

¹⁶C. W. Gardiner, *Handbook of Stochastic Methods: For Physics, Chemistry, and the Natural Sciences*, 3rd ed. (Springer, New York, 2004).